Low Temperature Physics/Fizika Nizkikh Temperatur, 2017, v. 43, No. 11, pp. 1642–1646

EPR studies of the triangular-lattice antiferromagnet Cs_2CuBr_4

E. Schulze[1,2], A.N. Ponomaryov[1], J. Wosnitza[1,2], H. Tanaka[3], and S.A. Zvyagin[1]

[1]*Dresden High Magnetic Field Laboratory (HLD-EMFL)*
Helmholtz-Zentrum Dresden-Rossendorf, D-01328 Dresden, Germany
E-mail: s.zvyagin@hzdr.de

[2]*Institut für Festkörperphysik, TU Dresden, D-01069 Dresden, Germany*

[3]*Tokyo Institute of Technology, Tokyo 152-8550, Japan*

Received June 19, 2017, published online September 25, 2017

The spin dynamics of the spin-1/2 triangular-lattice antiferromagnet Cs_2CuBr_4 is probed by means of high-frequency electron paramagnetic resonance (EPR) spectroscopy. Temperature dependences of EPR parameters are studied in a broad temperature range between 1.4 and 200 K for different orientations of the applied magnetic field. In the high-temperature regime ($T >> J/k_B$), an unusually broad and anisotropic resonance line is detected, suggesting a sizeable Dzyaloshinskii–Moriya interaction. Employing the theory of exchange narrowing, the ratio of the Dzyaloshinskii–Moriya vector components, $D_c/D_a \approx 0.3$, is estimated.

PACS: 75.50.Ee Antiferromagnetics;
76.30.–v Electron paramagnetic resonance and relaxation;
76.50.+g Ferromagnetic, antiferromagnetic, and ferrimagnetic resonances; spin-wave resonance.

Keywords: antiferromagnet, EPR, Dzyaloshinskii–Moriya interaction.

A spin-1/2 Heisenberg antiferromagnet (AF) on a triangular lattice is one of the best model systems to probe effects of quantum fluctuation and frustrations in strongly correlated spin systems, exhibiting unusual ground-state properties and a rich excitation spectrum. It was suggested, that quantum fluctuations can be strong enough to destroy the classical 120° order in triangular-lattice spin-1/2 Heisenberg AFs [1], resulting in a two-dimensional (2D) spin liquid with the excitation spectrum formed by fractionalized quasiparticles, spinons. Although the existence of such a 2D spin liquid has been predicted more than four decades ago, theoretical identification and experimental detection of this state of matter has proved challenging.

In general, the Hamiltonian of a spin-1/2 systems with a triangular lattice in zero field is given by

$$\mathcal{H} = J \sum_{\langle i,j \rangle} \mathbf{S}_i \cdot \mathbf{S}_j + J' \sum_{\langle i,j' \rangle} \mathbf{S}_i \cdot \mathbf{S}_{j'} + \mathcal{H}_\delta, \qquad (1)$$

where $\mathbf{S}_i$, $\mathbf{S}_j$, and $\mathbf{S}_{j'}$ are spin-1/2 operators at sites i, j, and j', respectively, J and J' are the exchange-coupling parameters along the horizontal and zigzag bonds [Fig. 1(a)], respectively, and $\mathcal{H}_\delta$ represents various possible small anisotropic contributions. Depending on the J'/J ratio, theory [2–7] predicts a rich variety of magnetic structures, ranging from the 1D collinear phase to an incommensurate triangular order.

The spin-1/2 triangular-lattice AFs Cs_2CuCl_4 and Cs_2CuBr_4 are among the most intensively studied representatives of this class of low-D frustrated materials. These two materials have many common properties. Both have a slightly distorted layered arrangement of Cu^{2+} ions in a triangular pattern [Fig. 1(b)]. The materials are character-

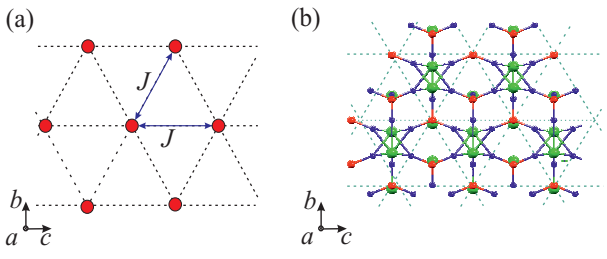

Fig. 1. (Color online) Schematic picture of exchange paths in Cs_2CuBr_4 in the *bc* plane (a). Schematic view of the crystal structure of Cs_2CuBr_4 in the *bc* plane. The Cu^{2+} ions form the triangular lattice. Red circles represent copper ions, while green and blue circles represent cesium and bromine ions, respectively (b).

ized by the same scale of in-plane spin interactions, $J/k_B = 4.7$ K, $J'/J \simeq 0.3$ and $J/k_B = 14.9$ K, $J'/J \simeq 0.41$ for Cs_2CuCl_4 and Cs_2CuBr_4, respectively [8,9]. Due to finite interplane interactions, Cs_2CuCl_4 and Cs_2CuBr_4 undergo transitions into magnetically ordered incommensurate states, at $T_N = 0.62$ and 1.4 K, respectively [10,11]. In spite of these (and many other) similarities, the magnetic properties of Cs_2CuBr_4 appear much richer, including 1/3 and 2/3 saturation magnetization plateaus [12] and a number of additional (still unidentified) field-induced phase transitions [13]. Most importantly, the observation of a relatively large zero-field energy gap, $\Delta \sim 0.7J$, in the excitation spectrum of Cs_2CuBr_4 [9,14] appears to be inconsistent with the 1D scenario, proposed for Cs_2CuCl_4 [15,16]. One of the critical issues is to clarify the reason for such a big difference of the magnetic properties of these two frustrated materials.

Electron paramagnetic resonance (EPR, also known as electron spin resonance, ESR) spectroscopy is recognized as a very powerful tool to probe the anisotropy of magnetic interactions in strongly correlated spin systems. Recently performed EPR studies of Cs_2CuCl_4 [17] provided the important information on the magnetic anisotropy in this material. It was shown that the main source of the high-temperature EPR line broadening is the Dzyaloshinskii–Moriya (DM) interaction. Employing a high-temperature approximation, the vector components of the DM interaction, $D_a = 0.33$ K and $D_c = 0.36$ K, were determined from the EPR angular dependence in the *ac* plane.

Cs_2CuBr_4 realizes a distorted triangular lattice with orthorhombic crystal structure (space group *Pnma*) and the room-temperature lattice parameters $a = 10.195$ Å, $b = 7.965$ Å, $c = 12.936$ Å, and $Z = 4$ (the number of formula units per unit cell) [18]. High-quality single crystals of Cs_2CuBr_4 were grown by slow evaporation of aqueous solutions of CsBr and $CuBr_2$ similar as described in [18]. Due to a relatively broad line, no resonance absorption was detected using the standard *X*-band EPR spectrometer. The EPR measurements were performed employing a high-frequency transmission-type spectrometer equipped with a 16 T superconducting magnet, similar to that described in Ref. 19. A VDI modular transmitter (product of Virginia Diodes Inc., USA) was used as a mm-wave radiation source. The EPR measurements were performed at temperatures down to 1.4 K.

The temperature dependences of the EPR linewidth and effective *g* factors measured at a frequency of 312 GHz for three field orientations are shown in Figs. 2 and 3, respectively. One can see that the linewidth and *g* factor do not show any significant temperature dependence down to approximately 40–50 K. Below this temperature, the EPR field shifts and line broadening is observed. Such a behavior is an indication of the combined effect of exchange and anisotropic spin-spin interactions. At approximately 14 K, the EPR line splits (the splitting was

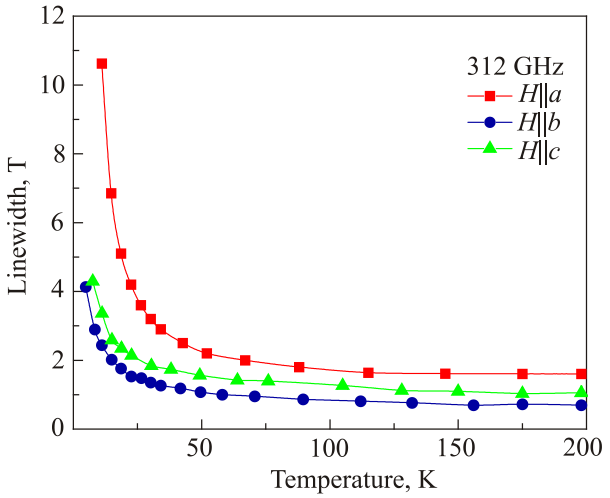

Fig. 2. (Color online) Temperature dependence of the EPR linewidths measured at 312 GHz. The data for $H \parallel a,b$ and c are labeled by squares, circles, and triangles, respectively. The lines are guides for the eye.

observed for $H \parallel a$, c; some selected spectra for $H \parallel a$ are shown in Fig. 4), eventually opening a gap, $\Delta \approx 9.5$ K, in the excitation spectrum [9,14]. From comparison to results of harmonic spin-wave theory calculations for the spin-1/2 triangular AF model (with parameters as defined in Ref. 9) the observed gapped mode was identified as a magnetic excitation at the Brillouin zone boundary, which is observable in Cs_2CuBr_4 due to the staggered DM interaction [14].

Above approximately 50 K, the system is in the high-temperature regime ($T >> J/k_B$). Remarkably, the EPR linewidth is almost constant at least up to 200 K, suggesting that the phonon-assisted spin-lattice broadening (which should be proportional to the temperature) is not relevant.

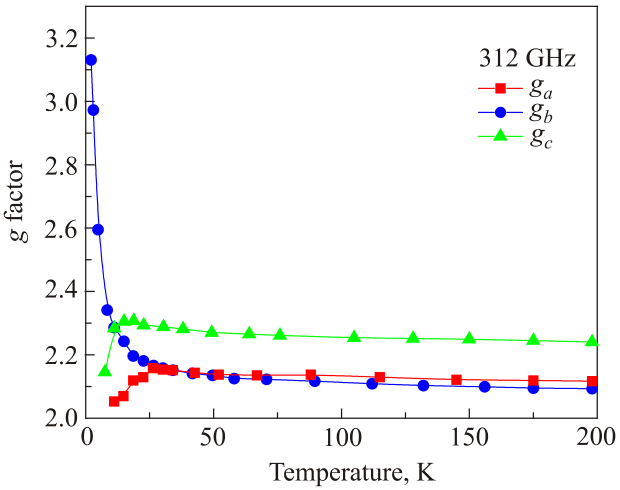

Fig. 3. (Color online) Temperature dependence of the effective *g* factor measured at 312 GHz. The data for $H \parallel a, b$ and c are labeled by squares, circles, and triangles, respectively. Note that data for $H \parallel a, c$ are shown only down to 14 K (below this temperature the EPR lines split). The lines are guides for the eye.

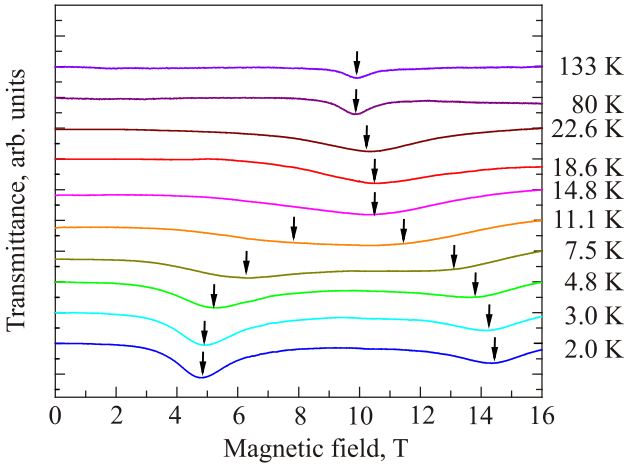

Fig. 4. (Color online) Selected EPR spectra measured at 312 GHz at different temperatures, $H \parallel a$. Resonance absorption maxima are denoted by arrows.

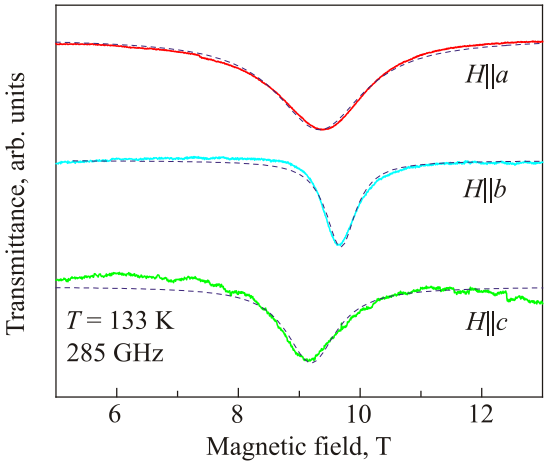

Fig. 5. (Color online) EPR spectra measured at 285 GHz, T = 135 K, with magnetic field applied along the three different crystallographic axes. The dashed lines are Lorentzian fit results.

Three spectra obtained at a frequency of 285 GHz for different field orientations (T = 135 K) are shown in Fig. 5. The spectra were fit using the Lorentzian line shape, revealing g_a = 2.17(2), g_b = 2.10(2), g_c = 2.22(2) and EPR full widths at half maximum (FWHM) ΔH_a = 1.75(1) T, ΔH_b = 0.60(1) T, ΔH_c = 1.00(3) T for $H \parallel a$, b, and c, respectively. It is important to mention, that contrary to many other spin-1/2 exchange-coupled spin systems with spin interactions of the same order of magnitude [20–23], the high-temperature EPR line in Cs_2CuBr_4 is up to two orders of magnitude broader (for comparison, the EPR linewidth in the isostructural compound Cs_2CuCl_4 measured at T = 100 K is ~0.02–0.03 T [17], which is about 50 times smaller than the EPR linewidth in Cs_2CuBr_4). Let us discuss possible contributions, which affect the EPR linewidth.

(i) Following the conventional estimates [24] and assuming that the distance between neighboring Cu^{2+} ions is ~8 Å, the contribution to the dipole-dipole interaction appears to be negligibly small (~1 Oe).

(ii) The anisotropic Zeeman contribution can be calculated using the equation [25]

$$\Delta H_{AZ} = \left(\frac{\Delta g}{g}\right)^2 \frac{g\mu_B H_{\rm res}^2}{\sqrt{\langle J^2\rangle}}, \qquad (2)$$

where $\Delta g = g_c - g_b$, $g = g_{a,c}$, and $\langle J^2\rangle = \frac{1}{3}(J^2 + 2J'^2)$ or $\langle J\rangle \approx 10$ K. As result, one obtains $\Delta H_{AZ} \approx 0.04$ T, which is much smaller than the measured EPR linewidth.

(iii) Rough estimates of two remaining major contributions to the EPR linewidth, the antisymmetric DM interaction and symmetric anisotropic interaction, give $D \propto (\Delta g/g)\langle J\rangle = 1.65$ K and $E \propto (\Delta g/g)^2\langle J\rangle = 0.2$ K, respectively [26]. Based on that, the DM interaction can be regarded as the main reason of the broad anisotropic EPR line observed in our experiments.

Figure 6 shows the angular dependence of the EPR linewidth with magnetic field applied in the ac plane, obtained at 312 GHz and T = 80 K.

If the EPR line is of Lorentzian shape, the FWHM ΔH can be calculated employing the theory of exchange narrowing [27] as

$$\Delta H = 2C\left(\frac{M_2^3}{M_4}\right)^{1/2}, \qquad (3)$$

where M_2 and M_4 are the second and fourth moment, C is a dimensionless constant, $C = \pi/\sqrt{2}$ [17]. Following the approach from Ref. 17, 27, the FWHM can be written as

$$\Delta H = C\frac{D^2(\alpha,\beta)k_B}{\langle J\rangle g\mu_B}\frac{1}{\sqrt{2}}. \qquad (4)$$

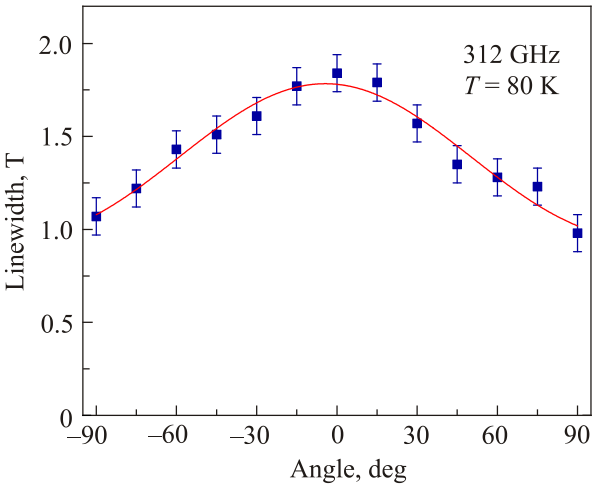

Fig. 6. (Color online) Angular dependence of the EPR linewidth with magnetic field applied in the ac plane, obtained at 312 GHz, T = 80 K. 0° corresponds to $H \parallel a$, while ±90° correspond to $H \parallel c$. The line is a guide for the eye.

Here, k_B is the Boltzmann constant, μ_B is the Bohr magneton, and

$$\mathcal{D}^2(\alpha,\beta) = D_a^2\left(1+\sin^2\beta\cos^2\alpha\right)+D_c^2\left(1+\cos^2\beta\right)+ +D_aD_c\cos\alpha\sin 2\beta, \quad (5)$$

where D_a and D_c are the DM vector components along the a and c axes, respectively. The angles α and β are defined by

$$\cos\alpha=\frac{A}{\sqrt{A^2+B^2}},\qquad \cos\beta=\frac{C}{\sqrt{A^2+B^2+C^2}},$$
$$A = g_{aa}\sin\theta\cos\varphi+g_{ab}\sin\theta\sin\varphi+g_{ac}\cos\theta, \quad (6)$$
$$B = g_{ca}\sin\theta\cos\varphi+g_{cb}\sin\theta\sin\varphi+g_{cc}\cos\theta.$$
$$C = g_{ba}\sin\theta\cos\varphi+g_{bb}\sin\theta\sin\varphi+g_{bc}\cos\theta,$$

Here, φ denotes the azimuthal angle counted from the a axis and θ denotes the polar angle counted from the c axis.

Taking into account that the magnetic field is applied in the ac plane (the DM interaction is not allowed along the b axis), we can neglect contributions to the moments for $\varphi\neq 0$. Our analysis provides $D_a = (4.7\pm0.5)$ K and $D_c = (1.6\pm0.3)$ K for the DM components along the a and c axes, respectively. These numbers appear to be too big, compared to $\langle J\rangle = 10$ K, questioning the validity of the used approach for compounds with a substantial DM interaction. Nevertheless, the approach can be employed for estimation of the D_c/D_a ratio. In our calculations, we neglect off-diagonal elements of the g tensor; the corresponding error due to each off-diagonal element does not exceed ~10%. Based on these considerations, the ratio D_c/D_a can be written as

$$\frac{\Delta H_c}{\Delta H_a}=\left(\frac{M_2^3(\varphi=0^\circ,\theta=0^\circ)/M_4(\varphi=0^\circ,\theta=0^\circ)}{M_2^3(\varphi=0^\circ,\theta=90^\circ)/M_4(\varphi=0^\circ,\theta=90^\circ)}\right)^{1/2}. \quad (7)$$

Using the function $\mathcal{D}^2$ as introduced in (5) and keeping $\varphi = 0^\circ$ fixed leads to

$$\left(\frac{M_2^3(\theta=0^\circ)/M_4(\theta=0^\circ)}{M_2^3(\theta=90^\circ)/M_4(\theta=90^\circ)}\right) = \left(\frac{\mathcal{D}^2(\theta=0^\circ)}{\mathcal{D}^2(\theta=90^\circ)}\right)^2 = \left(\frac{2D_c^2+D_a^2}{2D_a^2+D_c^2}\right)^2, \quad (8)$$

we obtain $D_c/D_a = 0.3(1)$.

In conclusion, we performed high-frequency EPR studies of the spin-1/2 triangular-lattice antiferromagnet Cs_2CuBr_4. In the high-temperature regime ($T >> J/k_B$), a very broad and anisotropic resonance line was detected, suggesting the presence of a sizeable DM interaction. Employing the EPR exchange narrowing theory, the ratio of the DM vector components, $D_c/D_a \approx 0.3$, was estimated. Our studies strongly suggest that the effect of the DM interaction is essential and needs to be taken into account, when explaining the cascade of the field-induced transitions and other unusual magnetic properties revealed in Cs_2CuBr_4 at low temperatures.

Acknowledgements

This work was supported by the Deutsche Forschungsgemeinschaft (DFG, Germany) and by the HLD at HZDR, member of the European Magnetic Field Laboratory (EMFL). The authors would like to thank M.S. Henriques for the help orienting samples.

1. P.W. Anderson, *Mater. Res. Bull.* **8**, 153 (1973).
2. O.A. Starykh, H. Katsura, and L. Balents, *Phys. Rev. B* **82**, 014421 (2010).
3. S. Ghamari, C. Kallin, S.S. Lee, and E.S. Sørensen, *Phys. Rev. B* **84**, 174415 (2011).
4. D. Heidarian, S. Sorella, and F. Becca, *Phys. Rev. B* **80**, 012404 (2009).
5. M.Q. Weng, D.N. Sheng, Z.Y. Weng, and R.J. Bursill, *Phys. Rev. B* **74**, 012407 (2006).
6. A. Weichselbaum and S.R. White, *Phys. Rev. B* **84**, 245130 (2011).
7. J. Reuther and R. Thomale, *Phys. Rev. B* **83**, 024402 (2011).
8. R. Coldea, D.A. Tennant, K. Habicht, P. Smeibidl, C. Wolters, and Z. Tylczynski, *Phys. Rev. Lett.* **88**, 137203 (2002).
9. S.A. Zvyagin, D. Kamenskyi, M. Ozerov, J. Wosnitza, M. Ikeda, T. Fujita, M. Hagiwara, A.I. Smirnov, T.A. Soldatov, A.Y. Shapiro, J. Krzystek, R. Hu, H. Ryu, C. Petrovic, and M.E. Zhitomirsky, *Phys. Rev. Lett.* **112**, 077206 (2014).
10. R. Coldea, D.A. Tennant, R.A. Cowley, D.F. McMorrow, B. Dorner, and Z. Tylczynski, *J. Phys. Condens. Matter* **8**, 7473 (1996).
11. T. Ono, H. Tanaka, H. Aruga Katori, F. Ishikawa, H. Mitamura, and T. Goto, *Phys. Rev. B* **67**, 104431 (2003).
12. T. Ono, H. Tanaka, O. Kolomiyets, H. Mitamura, F. Ishikawa, T. Goto, K. Nakajima, A. Oosawa, Y. Koike, K. Kakurai, J. Klenke, P. Smeibidle, M. Meissner, R. Coldea, A.D. Tennant, and J. Ollivier, *Theor. Phys. Suppl.* **159**, 217 (2005).
13. N.A. Fortune, S.T. Hannahs, J. Yoshida, T.E. Sherline, T. Ono, H. Tanaka, and Y. Takano, *Phys. Rev. Lett.* **102**, 257201 (2009).
14. S.A. Zvyagin, M. Ozerov, D. Kamenskyi, J. Wosnitza, B.J. Krzystek, D. Yoshizawa, M. Hagiwara, R. Hu, H. Ryu, C. Petrovic, and M.E. Zhitomirsky, *New J. Phys.* **17**, 113059 (2015).
15. M. Kohno, O.A. Starykh, and L. Balents, *Nat. Phys.* **3**, 790 (2007).
16. K.Yu. Povarov, A.I. Smirnov, O.A. Starykh, S.V. Petrov, and A.Ya. Shipiro, *Phys. Rev. Lett.* **107**, 037204 (2011).
17. M.A. Fayzullin, R.M. Eremin, A. Dittl, N. van Well, F. Ritter, W. Aßmus, J. Deisenhofer, H.-A. Krug von Nidda, and A. Loidl, *Phys. Rev. B* **88**, 174421 (2013).

18. B. Morosin and E.C. Lingafelter, *Acta Crystallogr*. **13**, 807 (1960).
19. S.A. Zvyagin, J. Krzystek, P.H.M. van Loosdrecht, G. Dhalenne, and A. Revcolevschi, *Physica B* **346–347**, 1 (2004).
20. B. Pilawa, *J. Phys.: Condens. Matter* **9**, 3779 (1997).
21. H.-A. Krug von Nidda, L.E. Svistov, M.V. Eremin, R.M. Eremina, A. Loidl, V. Kataev, A. Validov, A. Prokofiev, and W. Aßmus, *Phys. Rev. B* **65**, 134445 (2002).
22. A.A. Validov, M. Ozerov, J. Wosnitza, S.A. Zvyagin, M.M. Turnbull, C.P. Landee, and G.B. Teitel'baum, *J. Phys.: Condens. Matter* **26**, 026003 (2014).
23. V.N. Glazkov, M. Fayzullin, Yu. Krasnikova, G. Skoblin, D. Schmidiger, S. Mühlbauer, and A. Zheludev, *Phys. Rev. B* **92**, 184403 (2015).
24. I. Yamada, M. Nishi, and J. Akimutsu, *J. Phys.: Condens. Matter* **8**, 2625 (1996).
25. D.L. Huber, G. Alejandro, A. Caneiro, M.T. Causa, F. Prado, M. Tovar, and S.B. Oseroff, *Phys. Rev. B* **60**, 12155 (1999).
26. T. Moriya, *Phys. Rev. B* **120**, 92 (1960).
27. T.G. Castner, Jr. and M.S. Seehra, *Phys. Rev. B* **4**, 38 (1971).